

Super Resolution Perception of Industrial Sensor Data

Jinjin Gu, Haoyu Chen, Guolong Liu, Gaoqi Liang, Xinlei Wang, Junhua Zhao*
{jinjingu,haoyuchen,guolongliu,xinleiwang}@link.cuhk.edu.cn,{gaoqiliang,zhaojunhua}@cuhk.edu.cn
School of Science and Engineering, The Chinese University of Hong Kong, Shenzhen
Shenzhen, China

ABSTRACT

In this paper, we present the problem formulation and methodology framework of Super-Resolution Perception (SRP) on industrial sensor data. Industrial intelligence relies on high-quality industrial sensor data for system control, diagnosis, fault detection, identification, and monitoring. However, the provision of high-quality data may be expensive in some cases. In this paper, we propose a novel machine learning problem – the SRP problem as reconstructing high-quality data from unsatisfactory sensor data in industrial systems. Advanced generative models are then proposed to solve the SRP problem. This technology makes it possible to empower existing industrial facilities without upgrading existing sensors or deploying additional sensors. We first mathematically formulate the SRP problem under the Maximum a Posteriori (MAP) estimation framework. A case study is then presented, which performs SRP on smart meter data. A network, namely SRPNet, is proposed to generate high-frequency load data from low-frequency data. We further employ a novel recognition-based loss and relativistic adversarial loss to constraint the reconstruction of waveforms explicitly. Experiments demonstrate that our SRP model can reconstruct high-frequency data effectively. Moreover, the reconstructed high-frequency data can lead to better appliance monitoring results without changing the monitoring appliances.

KEYWORDS

Industrial system, Industrial sensors, Signal processing, Deep learning, Super-resolution

1 INTRODUCTION

Industry is a vital part of the economy that produces commodities in a centralized, mechanized, and automatized way. With the introduction of Industry 4.0, a new fundamental paradigm shift in industrial production is resulted from the combination of Internet technologies and emerging technologies in the field of ‘smart’ objects (machines and products) [21]. The rapid development of industrial intelligence will bring a tremendous impact on various fields of society.

Industrial intelligence is a key driver of the 4th Industrial Revolution, which can enable precise sensing and control of industrial systems through a large number of industrial sensors [1]. In the modern industry, in order to improve the operating efficiency and product quality, higher accuracy of sensing and control are essential. It will lead to a higher dependency on high precision and resolution data.

Collecting high-resolution state data of an industrial system is essential because of the following reasons. Firstly, many industrial systems, such as aero engines, chemical processes, manufacturing

systems, and power networks, are safety-critical systems. Reliability and safety are of utmost importance to these industrial systems, which, however, are vulnerable to potential process abnormalities and component faults [8]. Their tolerance to abnormality is very small, once small errors or abnormal fluctuations may cause serious consequences or losses. In practice, low-resolution state data may not be sufficient for detecting or rectifying system anomalies or faults. This may lead to permanent system damage or other potential security risks. For instance, a 1Hz frequency meter cannot measure the current overload that lasts less than 1s, the over-current event not detected by the low-frequency meters will lead to premature aging of the equipment and cause inestimable security risks. The inherent defects of low-frequency meters limit the capability of an industrial system to perceive and control its internal states in a more precise manner.

Secondly, accurate state monitoring is the basis for the optimization and control of an industrial system. In practice, the frequency of control actions is limited by the sampling frequency of meters. If the time interval between two control actions is too large, the economic efficiency or security of the system may be compromised. Take wind turbines as an example; the parameters of a wind turbine (e.g., blade angle) must be optimized according to the varying wind speed to increase the wind power output. If the time interval between two wind speed measurements is 5 minutes, it then means the wind power output of this turbine is not optimized within these 5 minutes. This is because the wind speed is constantly varying. The wind turbine is therefore not working in its optimal state.

In principle, installing higher-resolution meters is an ideal solution to the above problems. However, high-resolution meters have higher costs as well. On the other hand, this also means that a large number of low-resolution meters installed before have to be replaced, which is a huge waste of resources for large systems like power grids. Therefore, in this paper, we propose a novel machine learning problem, namely Super Resolution Perception (SRP). The proposed SRP problem aims at recovering high-resolution system state data from low-resolution data collected by the existing low-resolution meters, which can then be used to support more accurate and reliable state monitoring, optimization, and control.

There are at least four types of problems that can be solved by employing SRP. Firstly, without using high-resolution meters, SRP can support the high-resolution state monitoring of industrial systems. In practical industrial systems, sensors with different sampling frequencies may co-exist, which cannot satisfy the data quality requirement of precise control. By converting low-resolution data to higher resolution data, SRP provides a novel and practical way to solve this problem.

Secondly, the problem of bad data and data losses can also be improved by using SRP. It is very common that bad data are generated in some special cases during the operation of industrial systems,

*Junhua Zhao is the corresponding author

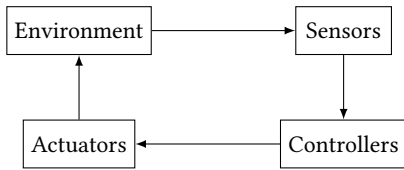


Figure 1: Flowchart of general control process.

or the measurement data are lost during transmission. Although state estimation and bad data detection, which are important components in industrial systems, can identify and eliminate bad data [3], the removed data cannot be supplemented, which therefore influences the accuracy of estimated system statuses. Through the detailed information provided by SRP, the bad data and missing data can not only be detected but also be well recovered, which contributes to any component that is operated based on collected data.

Thirdly, the security-constrained operation is vital for safety-critical industrial systems. In practice, every industry system must work in its specific security region, e.g., the temperature of a boiler must be maintained within a reasonable range. However, when the industrial sensors have insufficient sampling frequency, quality, and security variables will be difficult to measure [28]. This will lead to the risk that the system works in an unsafe state temporarily, which will compromise the lifetime and reliability of the system. The high-resolution data produced by SRP can help precisely control the state variables within the security regions and thus mitigate this kind of risk.

At last, high-precision control strategies require high-resolution data. The general flowchart of a control process is shown in Figure 1. Traditional industrial control systems (ICS) are based on mechanical or electrotechnical devices and closed systems. Today, these systems have become more expensive to deploy, maintain, and operate due to the higher functional requirements of modern industry. To address these challenges, more communication devices and sensors are being integrated into these systems, which in turn makes the systems more complex at the hardware level [18]. Different from relying on high-resolution sensors, SRP can reproduce high-resolution state data from low-resolution sensors and support the high-precision control (shown in Figure 2). This comes with almost no increase in system complexity and additional investments in sensors and communications.

1.1 Contributions

In summary, this paper introduces a novel machine learning problem called Super-Resolution Perception, to recover high-resolution industrial sensor data from low-resolution observations. Our main contributions in this paper are:

- We are among the first to propose the problem of SRP for industrial sensor data. Specifically, we propose a framework based on low-frequency sampling data to have a more precise perception of industrial systems.
- The method of applying deep learning to solve temporal dimension SRP, namely SRPNet, is proposed for the first time. Considering the security problems, such as power overload

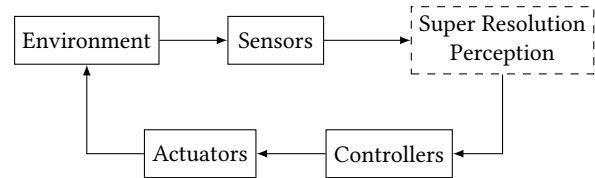


Figure 2: Flowchart of control process with SRP.

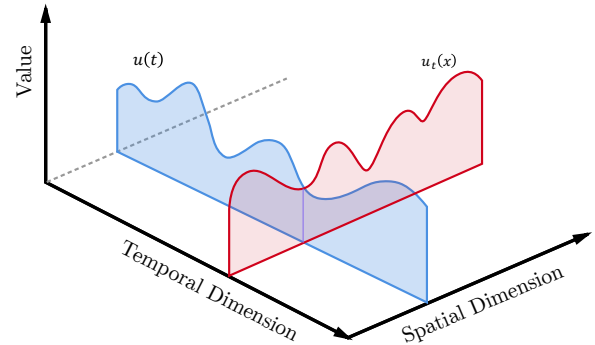


Figure 3: The relationship of temporal dimension and spatial dimension. When $u(t)$ is a scalar, u is a function of time t . When $u(t) = u_t(x)$ is a function of x in spatial dimension, u can be viewed as a multivariable function of t and x .

in industrial systems, this paper proposes a new feasible method to ensure the security of the system.

- To reconstruct the waveforms of high-frequency data accurately, we explicitly constraint the reconstruction of waveforms by employing a novel recognition-based loss and relativistic adversarial loss. Experiments demonstrated the effectiveness of the proposed objective functions.
- In this paper, we prove the value and effectiveness of SRP using smart meter data as a case study. Based on the high-resolution data produced by SRP, better control strategies and control effects can be achieved for smart grids.

1.2 Organization of the Paper

The remainder of the paper is organized as follows. Sec.2 presents the problem formulation and methodology framework of the proposed SRP on industrial sensor data. Sec.3 presents a real-world application of SRP on smart meter data. We then explore the potential of applying SRP in Non-Intrusive Load Monitoring and show the application value of SRP. At last, Sec.4 briefly discusses other potential applications of SRP and future work.

2 PROBLEM FORMULATION

Consider a continuous-space physical quantity u . The value of u at time t can be denoted by $u(t)$. Let l denote a low-resolution sensor data and h denote the high-resolution sensor data of the same physical quantity. The low-res data is generated from u by a continuous sampling function δ_L and the value of l at time period $[t_{start}, t_{end}]$ can be wrote as

$$l[t_n] = \int u(t)\delta_L(t - t_n)dt + n, t_n \in [t_{start}, t_{end}],$$

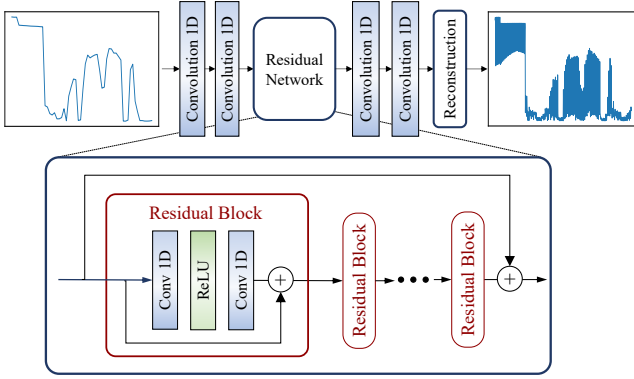


Figure 4: The proposed Super-resolution Perception Network (SRPNet). With two convolution layers for feature maps extraction, and a sub-pixel convolution layer that aggregates the feature maps from LR space and builds the SR image in a single step.

where n is noise. The high-res data h of same time period but with a finer grid is as

$$h[t_m] = \int u(t)\delta_H(t - t_n)dt + n, t_m \in [t_{start}, t_{end}],$$

where δ_H denote high-resolution sampling function and the time index t_m of h is more dense. Note that at same time t_0 , $h[t_0]$ and $l[t_0]$ may not equal because of the difference of δ_H and δ_L . Both l and h represent the value of the same physical quantity in the same time period, but h contains richer information on describing u . h and l are related by a degradation model:

$$l = \downarrow h + n,$$

where \downarrow is the degradation function and n is noise. SRP can be viewed as trying to inference h with l as input. SRP aims to find a reconstruction mapping f that the reconstructed high-res data $h' = f(l)$ that recovers the information lost by degradation function as much as possible.

The purpose of SRP is different depending on the property of u , and degradation function \downarrow . If the loss of information caused by degradation function is reflected in frequency reduction in the temporal dimension, the problem of restoring such temporal information is called *Temporal SRP* problem. According to different application scenarios, $u(t)$ can be a scalar or a function on spatial dimension $u(t) = u_t(x)$, where x denote the spatial position. If the degradation process loses the spatial information, the corresponding SRP problem is called *Spatial SRP* problem. The SRP problem considering both temporal and spatial dimensions is called *Spatial-Temporal SRP* problem. The relationship between the temporal and spatial dimension is shown by Figure 3. For different kinds of degradation functions, the SRP problem can be viewed as a superset of the various data quality problems, such as incomplete data, bad data, and malicious data, etc.

2.1 Interpretation of SRP as MAP estimation

We next show that the SRP can be viewed as Maximum a Posteriori (MAP) estimation. For a given low-res sensor data l , there are many possible h satisfying the degradation function. The final estimated

h is the solution with maximum posterior probability $p(h|l)$. According to the Bayesian formula, the posterior probability can be written as

$$p(h|l) = \frac{p(l|h)p(h)}{p(l)},$$

where $p(l|h)$ is the likelihood, $p(h)$ is the prior on h and $p(l)$ is a constant when l is given. The corresponding h given a specific l can be estimated by solving the MAP problem

$$h' = \arg \max_h p(h|l) = \arg \max_h p(l|h)p(h),$$

which is equivalent to solving the following formula

$$h' = \arg \max_h \log p(l|h) + \log p(h),$$

in which $p(l|h)$ can be solved by modeling the degradation process and $p(h)$ is obtained by solving the prior model. This indicates that the h estimated by the SRP should not only satisfy the degradation model but also satisfy the priori characteristics of h . The prior term $p(h)$ can be viewed as a regularization term. Effectively modeling the prior of h is important to SRP problems.

This also explains how SRP reconstructs information that is not collected by low-resolution data. There are two situations to this problem: (1) The low-res data did not record the event directly. However, an event will last for a period of time; it is thus possible to recover this event by relying on the part of the information produced by this event and recorded in low-res data. (2) The information of one event is completely lost. In this case, it is still possible to reasonably estimate the occurrence of an event by the prior knowledge of the event as long as the event is not independent. If one event is independent and the information is completely lost, this is beyond the capability of the proposed SRP.

3 CASE STUDY

In this paper, we study the SRP problem using smart meter data as an example. Smart meter data is collected by a single measurement unit (meter), and it records the overall electricity consumption of a household. This data can be used for monitoring, analysis, and identification of load. The frequency of the meter data depends on the sampling frequency of the smart meter. High-frequency meter data contains more information and can be better used for monitoring and analysis of electricity consumption. However, existing measurement units are mostly low-frequency units, which cannot produce high-frequency observation data directly. We use SRP to process low-frequency load data and reproduce possible high-frequency data with an end-to-end neural network SRPNet. We further prove that the use of estimated high-frequency data can lead to better appliance monitoring results without changing the monitoring method. In this case, the physical quantity $u(t)$ represents the instantaneous power at time t , which is a scalar. The load data in a certain period of time appears as a sequence. For a given time period, we denote the low-res load data collected by low-frequency meters as x with frequency f_l . The corresponding high-res data is y , and with a higher frequency of f_h . For a single meter, $x(t)$ is a scalar and $x \in \mathbb{R}^d$, d denote the length of low-res data. With a super-resolution factor α , we have $f_h = \alpha f_l$ and thus $y \in \mathbb{R}^{\alpha d}$. According to the degradation model, we have $x = \downarrow y + n$. Our goal is to recover y from x by a SRP mapping f .

3.1 Prior Works

We first review the prior works of the High-Resolution Data Generation. Due to the powerful approximation ability of deep neural networks, deep learning-based generative models have been widely used for data generation and processing. Deep generative models are also used in image super-resolution and audio super-resolution. Dong et al. [5] first train a three-layer convolutional neural network (CNN) for image super-resolution. In past years, various deep learning-based methods with different network architectures [12, 15, 16, 20, 30, 34, 35] and training strategies [7, 10, 11, 32] have been proposed to improve the SR performance continuously. Advanced machine learning methods are also used to super-resolve audio data. Dong *et al.* [6] learn an analysis dictionary from the spectrogram of some related audio signals. And then, the learned dictionary is then applied in a l_1 -norm regularization term for the reconstruction of the high-resolution spectrogram. Mandel *et al.* [26] utilize a non-linear dictionary-based denoising system to transform low-bandwidth, low-bitrate speech into high-bandwidth, high-quality speech. Kuleshov *et al.* [19] propose an encoder-decoder network to super-resolve audio data and achieve the state-of-the-art performance in reconstructing high resolution audios.

Although generative models have been very effective in many signal processing tasks, however, to the best of our knowledge, there is no such method designed to super-resolve industrial sensor data. Compared with audio super-resolution, the super-resolution factor of industrial sensor data are often 10, 100, or even 1000. It is much larger than that of audio, which only is 2, 5, or 10. Industrial sensor data usually contains more distinct patterns than natural audio data. These unique characteristics of industrial sensor data also make it possible to support large SRP factors such as 100 and 1000.

3.2 Method

We develop a deep convolutional neural network called SRPNet to implement the abovementioned mapping. In this section, we first present the network architecture of SRPNet. We next present the used objective function. At last, we present the training details of SRPNet.

3.2.1 Network Architecture. The network architecture of SRPNet is shown in Figure 4. SRPNet takes the low-frequency data as the input and outputs the estimated high-frequency data directly. At the top of the network, two 1D convolution layers are operated as a global feature extractor. This extractor extracts features from low-res input and represents the features as many feature vectors. These vectors contain the abstract feature information of input, and each vector has the same dimension as input data. After feature extraction, an information supplemental sub-network with the residual structure is used to supplement the lost information to the feature vectors. The residual structure consists of a big global residual connection and many local residual blocks. The global residual connection will force the network to learn the lost information rather than form the signal itself. The local residual blocks make it possible to train a deeper network [13]. In SRPNet, we use 16 local residual blocks for better performance. The third part is a reconstruction sub-network. In this part, the feature vectors are integrated into α sub-sequences $\phi \in \mathbb{R}^{\alpha \times d}$ by two 1D convolution layers. Then

rearrange the α channels of the same pixel of the sub-sequences into a new sequence of length α , corresponding to a α size sequence fragment in the high-res data. Thus the α sub-sequences with length d are rearranged into the estimated high-res sequence with length $\alpha \times d$. This sequence is expected to be similar to the ground truth y .

The proposed SRPNet is mainly distinguished from the existing time series data generation methods in two aspects: (1) Different from WaveNet [31], which uses a recursive strategy to generate sequence data, we use convolution operation to generate high-res sequences in parallel. This saves unnecessary calculations and provides higher computational efficiency when generating long sequences. For WaveNet, it takes about 60 minutes to generate 10000 samples. And it only takes 0.2 seconds for SRPNet to generate a sequence with the same length. (2) In SRPNet, the feature extraction and information supplement are performed on low-res sequences, and the upsampling function is implicitly included in the previous convolutional layers, which can be learned automatically. This not only reduces the computation complexity but also makes it easier to generate the desired waveform when SRP. Compared with AudioNet [19], which first upsample the sequences and then change the waveform with a neural network, SRPNet is able to perform SRP with higher SR factors, shorter running time, and better SR performance.

3.2.2 Objective Function. In the proposed method, the objective function consists of three parts. We first employ the l_2 -norm loss:

$$\mathcal{L}_2(y, y') = \|y - y'\|_2^2,$$

where y' indicates the generated high-resolution data. However, because the l_2 -norm loss contains square operation, the gap between the larger error and the smaller error will be enlarged. In other words, the l_2 -norm will punish the larger error strongly and will tolerate the smaller error. This brings difficult to reconstruct the waveform of the smart grid signal. What is more important is that we want the super-resolved data could help the subsequent downstream applications such as recognition and monitoring. In this case, the reconstruction of waveforms is practically essential.

In order to better reconstruct the waveforms and make the super-resolved data suitable for the subsequent monitoring application, we adapt a CNN based recognition network after the generation network as a recognition-based loss to explicitly constrain the reconstruction of waveforms. By calculating losses through the recognition network, it will force the SRPNet to generate waveforms that can be recognized by the recognition network correctly. This recognition loss is formulated as the cross-entropy loss between the predicted label and the ground truth label:

$$\mathcal{L}_{Rec}(y, y') = - \sum R(y') \log a + (1 - R(y')) \log(1 - a),$$

where R is the CNN recognition network, and a is the label vector indicating the running electric appliance of x . For each appliance, the label a is either 1 or 0, where the former indicates this appliance is sunning, and the later indicates the opposing situation. R is pretrained with the ground truth high-resolution data and is able to capture the crucial features that are important for recognition. We adapt cross-entropy loss to train the R network.

In addition to the above losses, we also adopt adversarial loss [22] to learn the HR data manifold for the long sequence from the

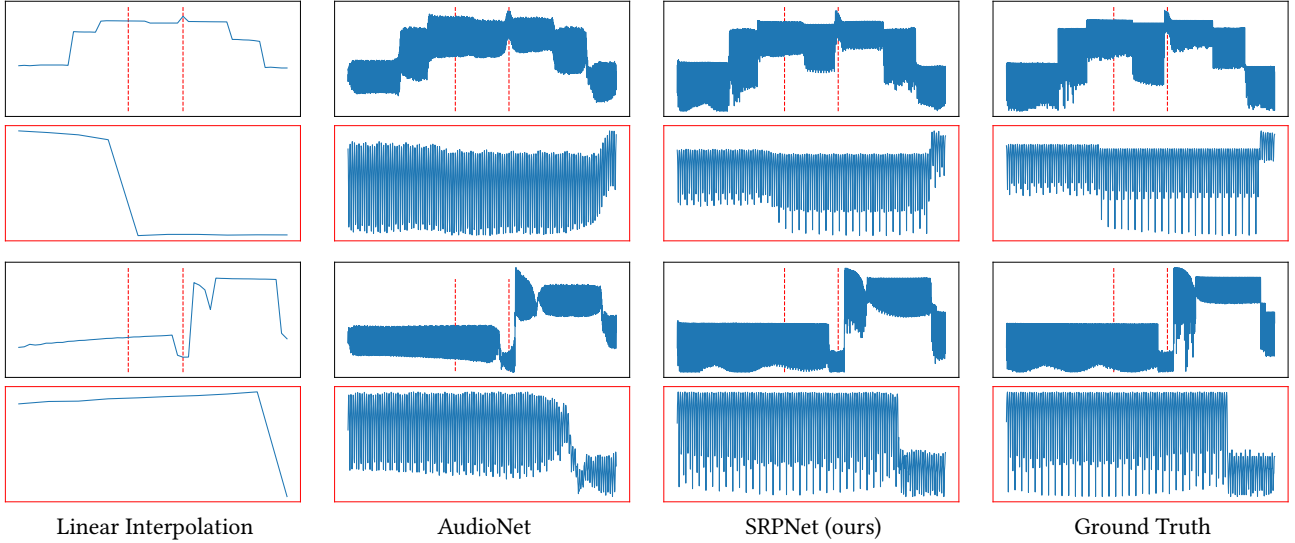


Figure 5: The SRP results of experiment with $f_l = 10\text{Hz}$ and $\alpha = 100$.

global perspective. The adversarial loss makes the generated long sequences close to the target manifold. The adversarial training strategy contains the generator and a discriminator. The goal of the discriminator is to try to separate the signals generated by the generator from the real ones. Ideally, the generator can generate signals with a realistic waveform that can deceive a well-trained discriminator. Inspired by ESRGAN [32], we change the standard GAN loss to Relativistic GAN loss [14]. Different from the standard discriminator D , which estimates the probability that one input y is on the target manifold, a relativistic discriminator tries to predict the probability that a real data y is relatively more realistic than a fake one y' . The standard discriminator can be expressed as $D(y) = \text{sigmoid}(C(y))$, where $C(y)$ is the discriminator output before any transformation. Then, the used Relativistic Discriminator D_{Ra} is formulated as:

$$D_{Ra}(y, y') = \text{sigmoid}(C(y) - \mathbb{E}_{y'}[C(y')]),$$

where $\mathbb{E}_{y'}$ represents the operation of taking the average for all fake HR data in one mini-batch. And the discriminator loss is then formulated as:

$$\mathcal{L}_D^{Ra} = -\mathbb{E}_y[\log(D_{Ra}(y, y'))] - \mathbb{E}_{y'}[\log(1 - D_{Ra}(y, y'))].$$

The adversarial loss for the SRP network $G(\cdot)$ is in a symmetrical form:

$$\mathcal{L}_G^{Ra} = -\mathbb{E}_y[\log(1 - D_{Ra}(y, y'))] - \mathbb{E}_{y'}[\log(D_{Ra}(y, y'))].$$

In this adversarial loss, both y and y' are contained explicitly. Thus the Relativistic GAN loss can consistently produce gradients close to the data manifold without being affected by the over-training of the discriminator.

The overall loss function used for our full methods is:

$$\mathcal{L} = \lambda_{sr} \cdot \mathcal{L}_2 + \lambda_{adv} \cdot \mathcal{L}_G^{Ra} + \lambda_{rec} \cdot \mathcal{L}_{Rec},$$

where λ_{sr} , λ_{adv} and λ_{rec} are the hyper-parameter of for content l_2 -norm loss, the adversarial loss and recognition loss, respectively.

3.2.3 Network training. For optimization, we use Adam [17] with $\beta_1 = 0.9$ and $\beta_2 = 0.999$. The mini-batch size is set to 32. For each batch, the data are randomly cropped into 10 seconds for the training. The learning rate is initialized as 1×10^{-4} for the first 1×10^6 mini-batch updates and then fine tuned with learning rate of 1×10^{-6} for another 1×10^6 mini-batch updates. For the hyper-parameter of objective function, we use $\lambda_{sr} = 1$, $\lambda_{adv} = 0.01$ and $\lambda_{rec} = 0.01$ for the best performance. The settings of the loss hyper-parameter will be discussed in the ablation study section. We implement our models with the PyTorch framework and train them using NVIDIA Titan Xp GPUs. The entire training process took about twenty hours.

3.3 Dataset and Data Preparation

We use the simulated smart meter data to train the proposed SRPNet and test it on real-world data. For the simulation data, we simulated the working state of electrical appliances in houses and then combined the corresponding electrical load data into a final smart meter data for a house according to the working state. The used electrical load data of appliance in different states is provided in the Plug-Level Appliance Identification Dataset (PLAID) [4]. PLAID can be used in appliance identification; it provides 1793 high resolution (30000HZ) meter data instances of 82 different appliances which belong to 11 different appliance types. In the experiment, we prepare 14000 high-frequency data samples of length 30s for training, and another 2000 data were used for validation. For the testing data, we collect real-world electricity load data where the main appliances are similar to the appliances in training data. The testing set contains 130 hours of data.

Since the electrical load data has a very large dynamic range ($10^{-3} - 10^6$), it is difficult for the neural network to directly process the input and output with such a large dynamic range. We pre-process the original large dynamic meter data with the following formula

$$\tilde{x} = \log_{100}(x \times 10^3 + 1).$$

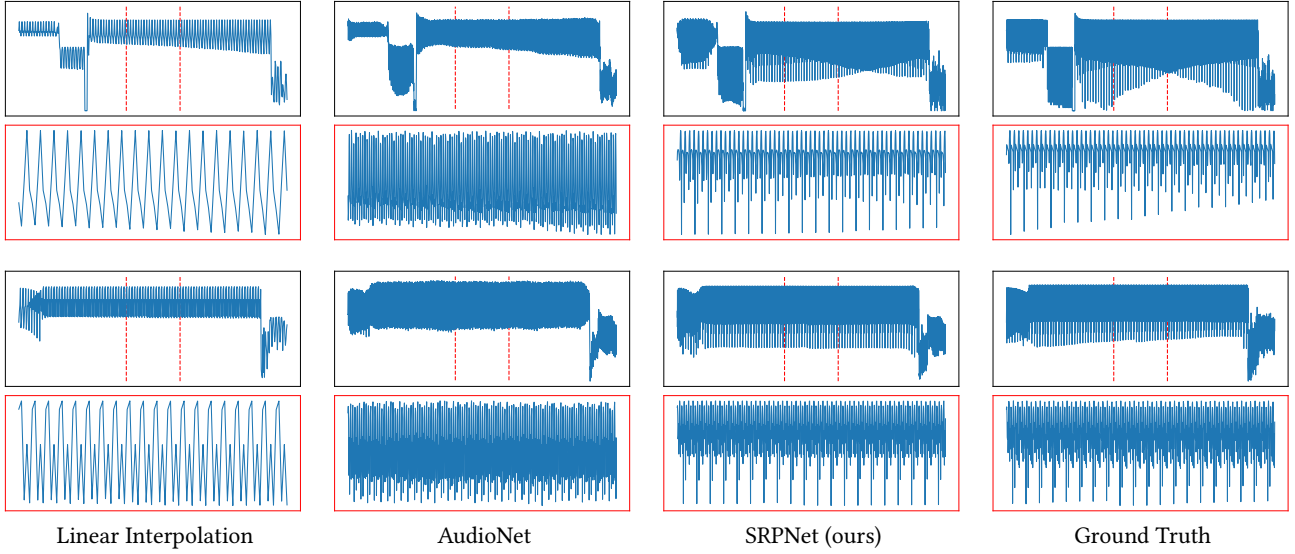


Figure 6: The SRP results of experiment with $f_l = 100\text{Hz}$ and $\alpha = 10$.

This formula is monotonous and ensured \tilde{x} to be positive. It well preserves the fluctuations in data. The high and low-frequency data used for training is based on the degradation model described in the problem formulation section. Since the meter records the instantaneous current and voltage values, we assume the sampled data given by the high-frequency meter and low-frequency meter are approximately equal. Thus, we employ the Nearest Neighbor (NN) down-sampling as the degradation function. Then, Gaussian noise with a $\sigma = 0.01$ was added to the down-sampled low-frequency data.

3.4 SRP Results

In order to study the characteristics and effectiveness of the proposed SRP method, we conducted experiments under three different settings: (1) the low-res data with frequency $f_l = 10\text{Hz}$ and an SRP factor of $\alpha = 10$; (2) $f_l = 100\text{Hz}$ and $\alpha = 10$; (3) $f_l = 10\text{Hz}$ and of $\alpha = 100$.

3.4.1 Quantitative Metrics. To quantify the comparison, we use two metrics: Signal to noise ratio (SNR) and The Log-spectral distance (LSD) [9]. SNR is a commonly used metric in the signal processing literature. Given a reference signal y and an approximation y' , the SNR is defined as

$$\text{SNR}(y, y') = 10 \times \log \frac{\|y\|_2^2}{\|y - y'\|_2^2}.$$

The LSD measures the reconstruction quality of individual frequencies as follows

$$\text{LSD}(y, y') = \frac{1}{L} \sum_{l=1}^L \sqrt{\frac{1}{K} \sum_{k=1}^K (X(l, k) - X'(l, k))^2},$$

where X and X' are the log-spectral power magnitudes of y and y' , respectively. These are defined as $X = \log \|S\|^2$, where S is the short-time Fourier transform of the signal. We use l and k index frames and frequencies, respectively. By combining the above metrics, we can evaluate the performance of temporal SRP methods.

3.4.2 Quantitative Comparison. We compared our method with linear interpolation, Li *et al.* [23], and AudioNet [19]. We also compared the performance of SRPNet using different losses. The quantitative comparison results are shown in the Table 1. It is obvious that the SRP method is significantly better than the existing methods. This experiment also demonstrates the effectiveness of the proposed recognition-based loss and adversarial loss. We can also find that the experiment of input frequency with 100hz and an SRP factor of 10 has the best SRP result. Because the high-frequency data contains more information on describing the real system state. Thus, it is easy for the generative model to infer the data before degradation. When the frequency of the input data becomes lower, the real system state is more difficult to estimate, and it is more difficult to recover high-frequency information therefrom. We can also see that when the SRP factor becomes 100, although the SRP can still recover the high-frequency data to a certain extent, it suffered more severe distortion than the experiment with an SRP factor of 10. These experiments demonstrate that: (1) when the input data has a lower frequency, it is more difficult to perform SRP; (2) it is more difficult to perform SRP with a larger super-resolution factor.

3.4.3 Qualitative Comparison. Since the existing traditional (not deep learning-based) time series upsampling methods (such as compressed sensing and dictionary learning) cannot perform SRP with SR factors of 10 or even 100, the comparison is conducted with linear interpolation and AudioNet [19]. Some SRP test results are shown in Figure 6 and Figure 5. For each sample, the first line of each case is the overview of a 5 second time slice, and the second line is the zoom-in view of 1 second marked by red lines in the overview. As can be seen, the interpolation method can not recover the missing details in the high-frequency data due to the loss of information during the degradation process. The AudioNet try to reconstruct waveforms with some high-frequency signals, yet the reconstruction is unreliable. Compared with our method, AudioNet can only restore the rough shape of the waveform; the details of the waveform are difficult to recover. However, the proposed SRP method can restore the waveforms and details effectively.

Method	$f_l = 10\text{Hz}, \alpha = 10$		$f_l = 100\text{Hz}, \alpha = 10$		$f_l = 10\text{Hz}, \alpha = 100$	
	SNR \uparrow	LSD \downarrow	SNR \uparrow	LSD \downarrow	SNR \uparrow	LSD \downarrow
Linear Interpolation	17.86	8.136	17.93	5.685	17.43	13.03
Li <i>et al.</i> [23]	20.21	2.718	28.24	2.021	20.08	2.569
AudioNet	25.93	2.253	35.83	1.279	23.21	3.109
SRPNet (l_2)	26.05	1.898	33.41	1.460	23.30	2.371
SRPNet (adv)	26.54	1.852	35.27	1.264	24.33	2.218
SRPNet (full model)	27.90	1.673	36.18	1.221	24.39	2.200

Table 1: The quantitative comparison of linear interpolation, AudioNet [19] and SRPNet (SNR / LSD). SRPNet (l_2) means using only l_2 -norm loss, SRPNet (adv) means training SRPNet with adversarial loss, and SRPNet (full model) indicates our full model including recognition-based loss. \uparrow means the higher the better while \downarrow means the lower the better.

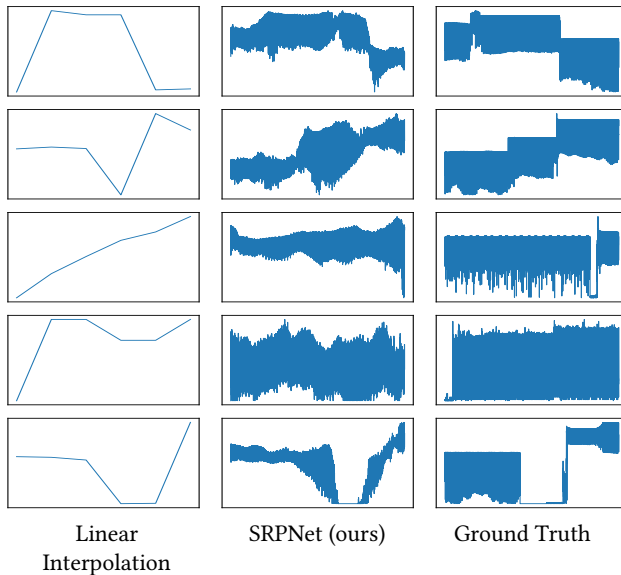


Figure 7: The SRP results of experiment with $f_l = 1\text{Hz}$ and $\alpha = 1000$.

Then we focus on some hard cases for the SRP problem: the low-resolution data with frequency $f_l = 1\text{Hz}$ and an SR factor of $\alpha = 1000$. Some examples are shown in Figure 7. The low-frequency data are 6 seconds slice of 1Hz smart meter data, which means there are only 6 data points. It is very difficult to restore the original waveform with extremely limited information. In this case, SRPNet can only recover part of the waveform information. The reconstructed signals have greater distortion compare to the ground truth. However, this experiment still shows the potential of applying SRP with a large SRP factor.

3.4.4 Ablation Study. To investigate the behaviors of these two losses, we conducted several ablation studies. First, we trained the network with only l_2 -norm loss as the baseline. Then, we added adversarial loss and recognition-based loss with different hyper-parameters to show how they affect the results. In this ablation study, the input frequency is 100hz, and the SRP factor is 10. The SRP results are shown in Figure 8. Table 2 shows the effect of adversarial loss. We can observe that the results using adversarial loss show better performance, and when $\lambda_{adv} = 0.01$, it achieves the best performance. Table 3 shows the effect of using

Method	$f_l = 10\text{Hz}, \alpha = 10$	
	SNR \uparrow	LSD \downarrow
$\lambda_{adv} = 0$	26.05	1.898
$\lambda_{adv} = 0.1$	26.28	1.889
$\lambda_{adv} = 0.01$	26.54	1.852
$\lambda_{adv} = 0.001$	26.48	1.886
$\lambda_{adv} = 0.0001$	26.23	1.893

Table 2: The quantitative comparison of different hyper parameters setting of SRPNet, λ_{sr} defaults to 1. \uparrow means the higher the better while \downarrow means the lower the better.

Method	$f_l = 10\text{Hz}, \alpha = 10$	
	SNR \uparrow	LSD \downarrow
$\lambda_{adv} = 0, \lambda_{rec} = 0$	26.05	1.898
$\lambda_{adv} = 0.1, \lambda_{rec} = 0.1$	27.32	1.785
$\lambda_{adv} = 0.1, \lambda_{rec} = 0.01$	27.72	1.730
$\lambda_{adv} = 0.1, \lambda_{rec} = 0.001$	27.10	1.783
$\lambda_{adv} = 0.01, \lambda_{rec} = 0.1$	27.76	1.695
$\lambda_{adv} = 0.01, \lambda_{rec} = 0.01$	27.90	1.673
$\lambda_{adv} = 0.01, \lambda_{rec} = 0.001$	27.71	1.722

Table 3: The quantitative comparison of different hyper-parameters setting of SRPNet (full model), λ_{sr} defaults to 1. \uparrow means the higher the better while \downarrow means the lower the better.

recognition-based loss. As one can see, the performance of the solution with recognition loss is generally better than the solution without recognition loss, and the performance is not sensitive to hyper-parameters. We can further observe that by combining adversarial loss and recognition loss, we can achieve the best performance when $\lambda_{adv} = 0.01$ and $\lambda_{rec} = 0.01$.

3.5 NILM Results

We then study the application of SRP in Non-Intrusive Load Monitoring (NILM). Appliance Load Monitoring (ALM) is essential for energy management solutions, allowing them to obtain appliance-specific energy consumption statistics that can further be used to devise load scheduling strategies for optimal energy utilization. NILM is the process of identifying appliances and their working states using a single smart meter. High-frequency data will increase the accuracy of NILM yet requires high-frequency smart meters which are more expensive. We use the SRP results as an alternative to high-frequency data.

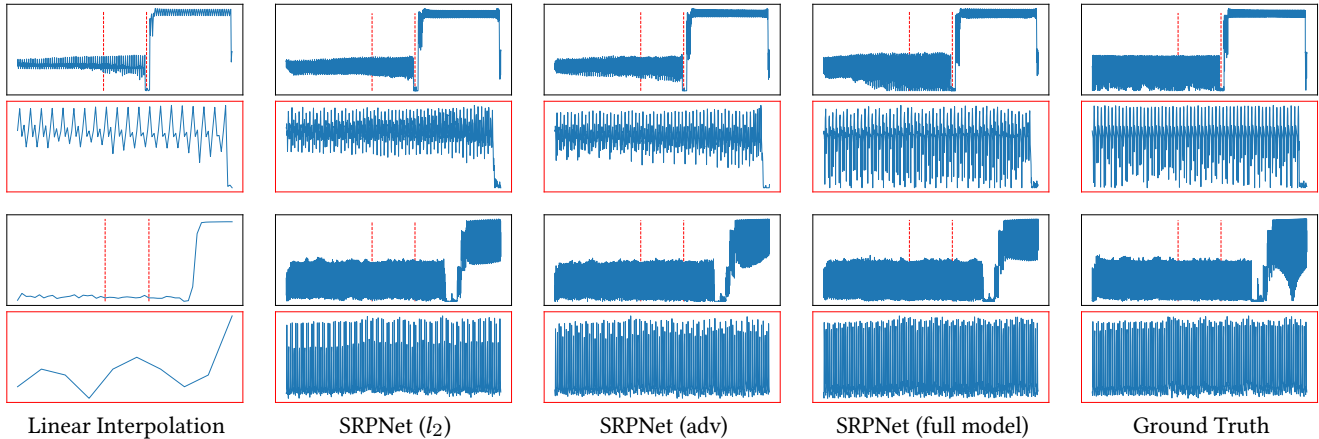


Figure 8: The first two rows are SRP results of experiment with $f_l = 100\text{Hz}$ and $\alpha = 10$, the third and fourth rows are SRP results of experiment with $f_l = 10\text{Hz}$ and $\alpha = 100$.

Method	Experiment	trained on LF test on LF	trained on HF test on SRPNet (l_2 only)	trained on HF test on SRPNet (full model)	trained on HF test on HF	Gain from SRPNet (l_2 only)	Gain from SRPNet (full model)
KNN	$f_l = 10\text{Hz}, \alpha = 10$	0.7703	0.7737	0.7779	0.7818	+0.0034	+0.0076
	$f_l = 100\text{Hz}, \alpha = 10$	0.7818	0.7917	0.7926	0.7939	+0.0098	+0.0108
	$f_l = 10\text{Hz}, \alpha = 100$	0.7703	0.7807	0.7898	0.7939	+0.0104	+0.0195
Decision Tree	$f_l = 10\text{Hz}, \alpha = 10$	0.6922	0.7056	0.7266	0.7332	+0.0134	+0.0344
	$f_l = 100\text{Hz}, \alpha = 10$	0.7332	0.7401	0.7421	0.7502	+0.0069	+0.0089
	$f_l = 10\text{Hz}, \alpha = 100$	0.6922	0.7225	0.7355	0.7502	+0.0303	+0.0433
MLP	$f_l = 10\text{Hz}, \alpha = 10$	0.8119	0.8202	0.8276	0.8332	+0.0083	+0.0157
	$f_l = 100\text{Hz}, \alpha = 10$	0.8332	0.8340	0.8347	0.8390	+0.0008	+0.0015
	$f_l = 10\text{Hz}, \alpha = 100$	0.8119	0.8198	0.8235	0.8390	+0.0079	+0.0116

Table 4: The accuracy results of NILM on different experimental settings. LF denotes low-frequency data and HF denotes high-frequency data.

Three classic NILM algorithms are used for this study: KNN [2], SVM [33] and Decision Tree [29]. For every algorithm and experiment setting, models are trained on both SRP results and high-frequency data and tested with SRP results. For comparison, the models trained and tested on low-frequency data and high-frequency data are used as a baseline. The accuracy results are shown in Table 4, which shows the reconstructed high-frequency data can lead to better appliance monitoring results without changing the monitoring appliances. Overall, the SRP results of the experiment with $f_l = 100\text{Hz}$ and $\alpha = 10$ have the best performance, which can increase the most accuracy among the three experiments. It will be very helpful for the industry to reduce energy consumption with low-resolution data sensors.

4 DISCUSSION AND FUTURE WORK

In this paper, we propose a novel machine learning problem - the SRP problem as reconstructing high-quality data from unsatisfactory sensor data in industrial systems. SRP can also be applied to many important industrial fields. State estimation (SE) is one of the most closely related scenarios. SE focuses on estimating system states at a specific time point. SRP will show good performances and play significant roles in the aforementioned area.

Industrial state estimation, as an important component of the industrial control process, is mainly performed to estimate system state variables under the state conditions characterized by a set of sensor measurements. Since most of the large-scale industrial systems are deployed decades ago, their state estimations are performed mainly based on low-frequency sampling sensors due to the limitations of sensor and communication technologies. However, the higher standards of modern industry on system efficiency and product quality require more accurate system state estimation. Also, a new source of threats, cyber attackers, are bringing significant challenges to the security of industrial control processes [24]. For example, Stuxnet targets industrial supervisory control and data acquisition (SCADA) systems and programmable logic controllers (PLC) to cause substantial system damages¹. Both industrial upgrade and security defense call for more precise monitoring on system running states, while existing low-frequency sampling sensors cannot meet the requirement.

Take the power system state estimation as an example. The power system state estimation is formulated as a non-convex optimization problem, which analyzes measurements of voltage and

¹See <https://en.wikipedia.org/wiki/Stuxnet> for more information.

power at certain nodes to output complete system states (including power, voltage magnitude, and angle) [27]. In the traditional power system, sensors (low-frequency) were deployed in the remote terminal units (RTUs), and some of the traditional sensors have been replaced by phasor measurement units (PMUs) (high-frequency) recently [25]. However, it is impossible to replace all traditional sensors with PMUs because PMU is extremely expensive. Under such circumstances, on the one hand, low-frequency measurements cannot provide high-resolution observations on system states; on the other hand, lots of high-frequency measurements collected from PMUs are wasted because the industry has no idea how to co-utilize both the high-frequency data collected by a small number of PMUs and the low-frequency data collected by traditional RTUs. This makes the power system state estimation a good application of SRP. SRP can supplement enough super-resolution information in between two sets of measurements so as to percept system states more clearly.

It should be noticed that different from the environment with only a single sensor, state estimation relies on multiple sensors at a specific time point to estimate corresponding state variables, which relies on the domain knowledge of system internal relationships in the space domain (e.g., the relationships between the temperatures of different rooms in a large building). Therefore, both the time domain and space domain information may be considered when applying SRP in industrial state estimation, which will be our future work.

REFERENCES

- [1] Michael Abramovici, Jens Christian Göbel, and Matthias Neges. 2015. Smart engineering as enabler for the 4th industrial revolution. In *Integrated systems: Innovations and applications*. Springer, 163–170.
- [2] Mario E Berges, Ethan Goldman, H Scott Matthews, and Lucio Soibelman. 2010. Enhancing electricity audits in residential buildings with nonintrusive load monitoring. *Journal of industrial ecology* 14, 5 (2010), 844–858.
- [3] NG Bretas, AS Bretas, and Andre CP Martins. 2013. Convergence property of the measurement gross error correction in power system state estimation, using geometrical background. *IEEE Transactions on Power Systems* 28, 4 (2013), 3729–3736.
- [4] Leen De Baets, Chris Develder, Tom Dhaene, Dirk Deschrijver, Jingkun Gao, and Mario Berges. 2017. Handling imbalance in an extended PLAID. In *2017 Sustainable Internet and ICT for Sustainability (SustainIT)*. IEEE, 1–5.
- [5] Chao Dong, Chen Change Loy, Kaiming He, and Xiaoou Tang. 2016. Image super-resolution using deep convolutional networks. *IEEE transactions on pattern analysis and machine intelligence* 38, 2 (2016), 295–307.
- [6] Jing Dong, Wenwu Wang, and Jonathon Chambers. 2015. Audio super-resolution using analysis dictionary learning. In *2015 IEEE International Conference on Digital Signal Processing (DSP)*. IEEE, 604–608.
- [7] Ruicheng Feng, Jinjin Gu, Yu Qiao, and Chao Dong. 2019. Suppressing model over-fitting for image super-resolution networks. In *Proceedings of the IEEE Conference on Computer Vision and Pattern Recognition Workshops*. 0–0.
- [8] Zhiwei Gao, Carlo Cecati, and Steven X Ding. 2015. A survey of fault diagnosis and fault-tolerant techniques—Part I: Fault diagnosis with model-based and signal-based approaches. *IEEE Transactions on Industrial Electronics* 62, 6 (2015), 3757–3767.
- [9] Augustine Gray and John Markel. 1976. Distance measures for speech processing. *IEEE Transactions on Acoustics, Speech, and Signal Processing* 24, 5 (1976), 380–391.
- [10] Jinjin Gu, Hannan Lu, Wangmeng Zuo, and Chao Dong. 2019. Blind super-resolution with iterative kernel correction. In *Proceedings of the IEEE conference on computer vision and pattern recognition*. 1604–1613.
- [11] Jinjin Gu, Yujun Shen, and Bolei Zhou. 2020. Image processing using multi-code gan prior. In *Proceedings of the IEEE/CVF Conference on Computer Vision and Pattern Recognition*. 3012–3021.
- [12] Muhammad Haris, Greg Shakhnarovich, and Norimichi Ukita. 2018. Deep back-projection networks for super-resolution. In *Conference on Computer Vision and Pattern Recognition*.
- [13] Kaiming He, Xiangyu Zhang, Shaoqing Ren, and Jian Sun. 2016. Deep residual learning for image recognition. In *Proceedings of the IEEE conference on computer vision and pattern recognition*. 770–778.
- [14] Alexia Jolicoeur-Martineau. 2018. The relativistic discriminator: a key element missing from standard GAN. *arXiv preprint arXiv:1807.00734* (2018).
- [15] Jiwon Kim, Jung Kwon Lee, and Kyoung Mu Lee. 2016. Accurate image super-resolution using very deep convolutional networks. In *Proceedings of the IEEE conference on computer vision and pattern recognition*. 1646–1654.
- [16] Jiwon Kim, Jung Kwon Lee, and Kyoung Mu Lee. 2016. Deeply-recursive convolutional network for image super-resolution. In *Proceedings of the IEEE conference on computer vision and pattern recognition*. 1637–1645.
- [17] Diederik P Kingma and Jimmy Ba. 2015. Adam: A method for stochastic optimization. In *ICLR*.
- [18] Siwar Kriaa, Ludovic Pietre-Cambacedes, Marc Bouissou, and Yoran Halgand. 2015. A survey of approaches combining safety and security for industrial control systems. *Reliability Engineering & System Safety* 139 (2015), 156–178.
- [19] Volodymyr Kuleshov, S Zayd Enam, and Stefano Ermon. 2017. Audio Super-Resolution Using Neural Nets. In *ICLR (Workshop Track)*.
- [20] Wei-Sheng Lai, Jia-Bin Huang, Narendra Ahuja, and Ming-Hsuan Yang. 2017. Deep laplacian pyramid networks for fast and accurate superresolution. In *IEEE Conference on Computer Vision and Pattern Recognition*, Vol. 2. 5.
- [21] Heiner Lasi, Peter Fetteke, Hans-Georg Kemper, Thomas Feld, and Michael Hoffmann. 2014. Industry 4.0. *Business & Information Systems Engineering* 6, 4 (2014), 239–242.
- [22] Christian Ledig, Lucas Theis, Ferenc Huszar, Jose Caballero, Andrew Cunningham, Alejandro Acosta, Andrew P Aitken, Alykhan Tejani, Johannes Totz, Zehan Wang, et al. 2017. Photo-Realistic Single Image Super-Resolution Using a Generative Adversarial Network.. In *CVPR*, Vol. 2. 4.
- [23] Kehuang Li and C. H. Lee. 2015. A deep neural network approach to speech bandwidth expansion. In *IEEE International Conference on Acoustics*.
- [24] Gaoqi Liang, Junhua Zhao, Fengji Luo, Steven R Weller, and Zhao Yang Dong. 2017. A review of false data injection attacks against modern power systems. *IEEE Transactions on Smart Grid* 8, 4 (2017), 1630–1638.
- [25] JBA London, Saulo Augusto Ribeiro Piereti, RAS Benedito, and NG Bretas. 2009. Redundancy and observability analysis of conventional and PMU measurements. *IEEE Transactions on Power Systems* 24, 3 (2009), 1629–1630.
- [26] Michael I Mandel and Young Suk Cho. 2015. Audio super-resolution using concatenative resynthesis. In *Applications of Signal Processing to Audio and Acoustics (WASPAA), 2015 IEEE Workshop on*. IEEE, 1–5.
- [27] A Monticelli. 2000. Electric power system state estimation. *Proc. IEEE* 88, 2 (2000), 262–282.
- [28] S Joe Qin. 2012. Survey on data-driven industrial process monitoring and diagnosis. *Annual reviews in control* 36, 2 (2012), 220–234.
- [29] Juan J Rodriguez and Carlos J Alonso. 2004. Interval and dynamic time warping-based decision trees. In *Proceedings of the 2004 ACM symposium on Applied computing*. ACM, 548–552.
- [30] Ying Tai, Jian Yang, Xiaoming Liu, and Chunyan Xu. 2017. Memnet: A persistent memory network for image restoration. In *Proceedings of the IEEE Conference on Computer Vision and Pattern Recognition*. 4539–4547.
- [31] Aäron Van Den Oord, Sander Dieleman, Heiga Zen, Karen Simonyan, Oriol Vinyals, Alex Graves, Nal Kalchbrenner, Andrew W Senior, and Koray Kavukcuoglu. 2016. WaveNet: A generative model for raw audio.. In *SSW*. 125.
- [32] Xintao Wang, Ke Yu, Shixiang Wu, Jinjin Gu, Yihao Liu, Chao Dong, Chen Change Loy, Yu Qiao, and Xiaoou Tang. 2018. ESRGAN: Enhanced Super-Resolution Generative Adversarial Networks. *arXiv preprint arXiv:1809.00219* (2018).
- [33] Yi Wu and Edward Y Chang. 2004. Distance-function design and fusion for sequence data. In *Proceedings of the thirteenth ACM international conference on Information and knowledge management*. ACM, 324–333.
- [34] Yulun Zhang, Kunpeng Li, Kai Li, Lichen Wang, Bineng Zhong, and Yun Fu. 2018. Image Super-Resolution Using Very Deep Residual Channel Attention Networks. *arXiv preprint arXiv:1807.02758* (2018).
- [35] Yulun Zhang, Yapeng Tian, Yu Kong, Bineng Zhong, and Yun Fu. 2018. Residual dense network for image super-resolution. In *The IEEE Conference on Computer Vision and Pattern Recognition (CVPR)*.